

Supplementary Information

Disorder-driven doping activation in organic semiconductors

Artem Fediai,^a Anne Emering,^a Franz Symalla^b and Wolfgang Wenzel^{*a}

^a Institute of Nanotechnology, Karlsruhe Institute of Technology, Hermann-von-Helmholtz-Platz 1, 76344, Germany. E-mail: wolfgang.wenzel@kit.edu

^b Nanomatch GmbH, Hermann-von-Helmholtz-Platz 1, 76344, Germany.

Content

S1. Weak and Strong Dopants	2
S2. Microscoping processes in doped organic materials	2
S3. Details of the model and simulated systems.	4
S4. Extraction of the average quantities from kMC simulations	5
Ionized dopant fraction Z	5
Density of states	5
S5. Appearance and positioning of the novel energy levels in a doped material with a weak dopant	6
S6. Material disorder as a function of doping	7
References	8

S1. Weak and Strong Dopants

Figure S1 visualizes the definitions of “weak” and “strong” dopant used in this work.

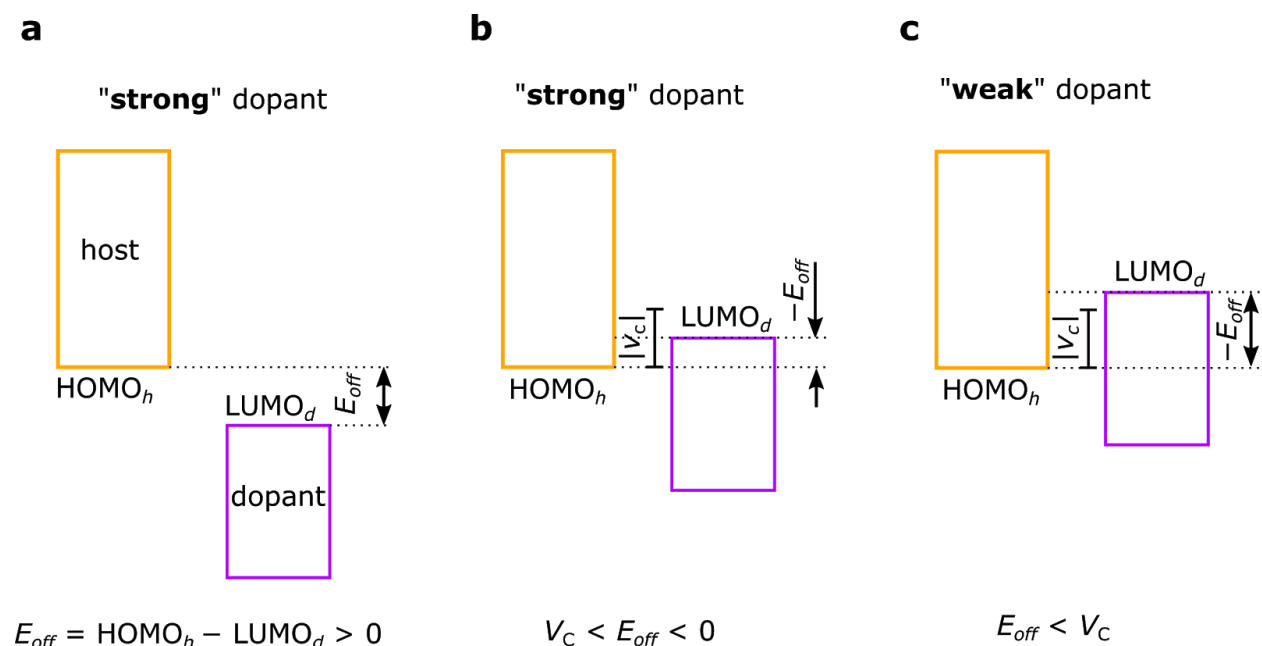
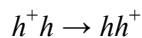


Figure S1. Energy diagram of the host and dopant pairs with various dopant “strengths”: (a) “strong” dopant (b) “strong” dopant often misinterpreted as a “weak” dopant, (c) “weak” dopant. At the bottom of the figure: conditions determining whether a dopant is denoted “weak” or “strong”. V_c is the Coulomb interaction energy of the host-dopant pair (negative).

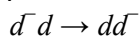
S2. Microscopic processes in doped organic materials

In our kMC simulations, four microscopic processes are considered:

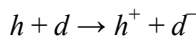
- (1) Hopping of a hole from one host molecule to another host molecule:



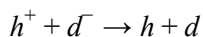
- (2) Hopping of an electron from one dopant molecule to another dopant molecule:



- (3) Dopant ionization:



- (4) Dopant neutralization:



Here, h and d stands for host and dopant molecules respectively, and the superscripts “+” and “-” denote the oxidation states of the molecules.

The rates of the processes (1)–(4) are described by Miller-Abrahams theory^[1], yielding the hopping rate of an electron/hole from site i to j , W_{ij}

$$W_{ij} = v_0 \exp(-2r/b) \exp\left[-\frac{|E_j - E_i| + (E_j - E_i)}{2k_B T}\right], \quad (\text{S1})$$

where E_j and E_i are the energies of the final and initial state, v_0 is the attempt-to-escape frequency, b is the localization radius of a charge carrier, k_B is Boltzmann constant, T is the temperature and r is the hopping distance. Host-dopant pair ionization is considered as a hop of a hole from the dopant LUMO to the host HOMO.

Energy of the final and initial states are defined by the difference of the corresponding frontier orbitals, and the energy of Coulomb interactions between ionized molecules if any. The energy difference $E_j - E_i$ has thus a stochastic contribution due to the intrinsic material disorder and doping-induced electrostatic disorder.

We note that the equilibrium state of the system (which is addressed in the manuscript) does not depend on the choice of the hopping rates as far as these obey the detailed balance principle. For instance, using Marcus rates^[2] instead of Miller-Abrahams rates does not change the results presented in the manuscript.

S3. Details of the model and simulated systems.

The parameters and assumptions we used in our simulations are summarized below:

1. Morphology: molecular sites are mapped to a cubic lattice with a lattice spacing of 1 nm. Dopants randomly substitute host molecules.
2. Number of hopping sites in the morphology: it depends on the doping concentration: from 10^6 sites for dopant concentration of 10^{-3} mol% down to 8×10^3 sites for 49 mol%. It has been checked for specific dopant concentrations (10^{-3} mol%, 10^{-2} mol%, 10^{-1} mol% and 10^{-3} mol%) that the doubling of the system sizes does not alter results.
3. Coulomb interactions: Coulomb interactions between all point charges are taken into account explicitly, without applying a cut-off. Moreover, we apply periodic boundary conditions in the level of so called nearest image convention, so that the interactions are computed not only between the molecules that belong to an actual simulation box, but also between the particles in this box and their nearest replicas.
4. Hopping range: hopping is possible to 25 nearest sites. Inverse localization radius b^{-1} is taken to be zero. Our computations have shown that this accelerates reaching the equilibrium state perhaps due to better sampling as a result for better connectivity of the sites. The attempt-to-jump frequency $\nu_0 = 10^{10}$ sec $^{-1}$. We note that the whole prefactor $\nu_0 \exp(-2r/b)$ and the range of the hopping (number of the nearest sites where the hopping is allowed to) does not change the time-averaged number of ionized dopants in the limit of the infinite Markov trajectory. As we only propagate the system for a finite number of steps, 10^6 , we regulated the prefactor in a way described above to provide the fast convergence to the relevant equilibrium microstates that allows for an efficient time averaging. All simulations are started from the microstate where all dopants are neutral.

S4. Extraction of the average quantities from kMC simulations

Ionized dopant fraction Z

The ionized dopant fraction, Z , analyzed in this manuscript is computed as a time-average along the kMC trajectory:

$$Z = 1/T \sum_i \tau_i Z_i,$$

where τ_i is the dwelling time at the i -th kmc frame, Z_i is the number of ionized dopants at this frame and $T = \sum_i \tau_i$. Simulations are started with all dopants being neutral. Time-averaging is performed over the second half of 10^6 kMC steps.

Density of states

In the manuscript, the densities of states of four orbitals are shown:

- (a) HOMO of the neutral host molecules, HOMO_h .
- (b) LUMO of the neutral dopant molecules, LUMO_d .
- (c) LUMO of the host cations, LUMO_h^+ .
- (d) HOMO of the dopant anion, HOMO_d^- .

These are formally introduced as the negative value of the corresponding binding energies, that is: $-\text{IP}_h$, $-\text{EA}_d$, $-\text{EA}_h^+$ and $-\text{IP}_d^-$, respectively.

The energy distribution of HOMO_h , LUMO_d , LUMO_h^+ and HOMO_d^- are determined as follows: at each i -th frame of the kMC trajectory we compute:

- (a) binned distribution of the $-\text{IP}_h$ of neutral hosts $\text{HOMO}_{h,i}(E)$,
- (b) binned distribution of the $-\text{EA}_d$ of neutral dopants $\text{LUMO}_{d,i}(E)$,
- (c) binned distribution of the $-\text{EA}_h^+$ of host cations $\text{LUMO}_{d,i}^+(E)$,
- (d) binned distribution of the $-\text{IP}_d^-$, of dopant anion $\text{HOMO}_{d,i}^-(E)$
- (e) dwelling time τ_i of the system at the i -th frame.

Time-averages of each of the orbitals distributions $D(E)$ with D standing for HOMO_h , LUMO_d , LUMO_h^+ or HOMO_d^- are then computed according to

$$D(E) = 1/T \sum_i \tau_i D_i(E),$$

where $T = \sum_i \tau_i$.

S5. Appearance and positioning of the novel energy levels in a doped material with a weak dopant

Figure 1 of the main text shows the computed energy level distributions and the nominal position of the HOMO/LUMO level of the host/dopant. **Figure S2** here provides a more detailed picture that explains the final positions of the levels, i.e. the shift by the Coulomb interaction and energy disorder. An analogous and even more detailed explanation for the less complicated case of a material with a fully ionized dopant is provided in [3].

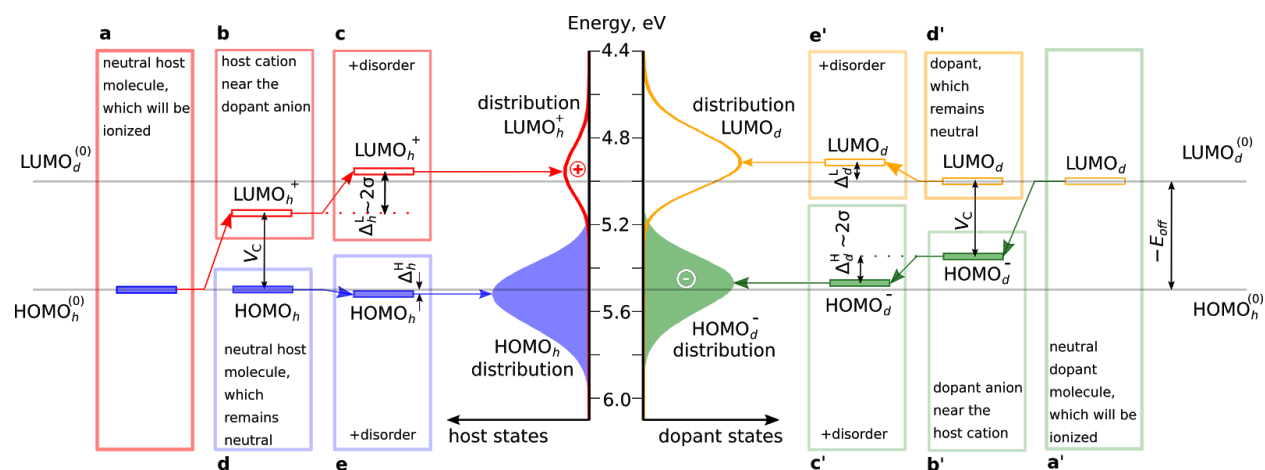


Figure S2. Appearance and positioning of the novel energy distributions of the material with a weak dopant (dopant molar ratio = 25 mol%, $E_{off} = V_C - 0.15$ eV, $\epsilon = 4$, $\sigma_{int} = 0.1$ eV). (a) HOMO of the host molecule, $HOMO_h$, which will later be ionized. (b) Upon ionization, the host cation preferably stays coulombically bound to the dopant anion whereby the mean of its LUMO, $LUMO_h^+$, is shifted up w.r.t the $HOMO_h$, by the amount of the Coulomb interaction energy V_C . (c) Due to the energy disorder, host molecules, which have their $HOMO_h$ in the upper part of the distribution, are preferentially ionized, leading to another upward shift of the mean $HOMO_h$ by $\Delta_h^L \approx 2\sigma$, with σ being the total energy disorder. This leads to the resulting distributions of $LUMO_h^+$ (central panel) shifted up w.r.t. $HOMO_h^{(0)}$ by $V_C + 2\sigma$. (a') LUMO of the dopant molecule, which will later be ionized. (b') Upon ionization, the dopant anion preferably stays coulombically bound to the host cation whereby its HOMO, $HOMO_d^-$, is shifted down w.r.t. the $LUMO_d$, by the amount of the Coulomb interaction energy V_C . (c') Due to energy disorder, dopant molecules, that have their $LUMO_d$ in the lower part of the distribution are preferentially ionized, leading to another downward shift of the mean $LUMO_d$ by $\Delta_d^H \approx 2\sigma$, with σ being the total energy disorder. This leads to the resulting distributions of $HOMO_d^-$ (central panel) shifted w.r.t. $LUMO_d^{(0)}$ down by $V_C + 2\sigma$. The mean values of the energy distributions of the host and dopant molecules that remain neutral, $HOMO_h$ (d) and $LUMO_d$ (d'), change as well. As long as $\sim 50\%$ of the dopant molecules are ionized and the ionized molecules come from the lower part of the $LUMO_d$, the mean value of the remaining $LUMO_d$ distributions is shifted up by $\Delta_d^L \approx 2\sigma$ (e). A similar but weaker effect is observed for $HOMO_h$: as far as the host molar rate is only 75%, only 12.5% of the host molecules are ionized (cf. with 50% of the ionized dopants). Therefore, we observe only a small shift of the mean $HOMO_h$ downwards, marked as Δ_h^H (e').

S6. Material disorder as a function of doping

Figure S2 shows the total disorder σ_{tot} (that is the standard deviation of the host HOMO distribution), additional energetic disorder defined as $\sigma_{tot} - \sigma_{int}$ and total disorder $\sqrt{\sigma_{tot}^2 - \sigma_{int}^2}$, assuming that the intrinsic and doping-induced disorder do not correlate, as a function of the dopant molar ratio. Plots are computed for materials with various dielectric permittivities ($\epsilon = [2, 3, 4]$) and intrinsic material disorders ($\sigma_{int} = [0.0, 0.1, 0.2]$ eV). In all cases, it is important to note that the additional disorder due to doping (**Figure S2b**) *decreases* as the intrinsic material disorder *increases*, that is low-disordered materials are more sensitive to the doping-induced disorder. Note that all plots are obtained for the case of a fully ionized dopant.

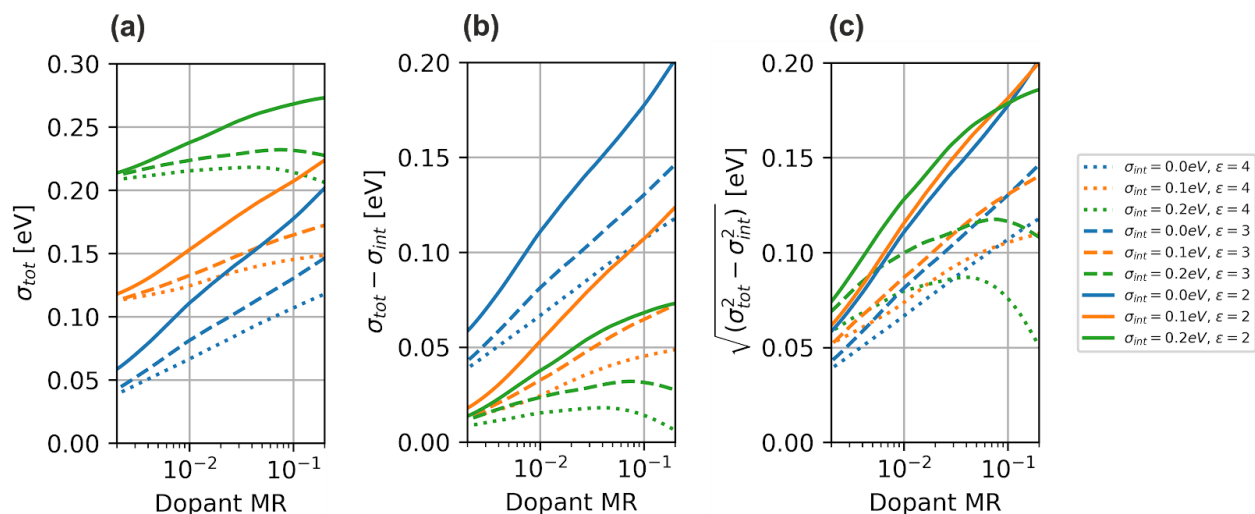


Figure S2. Material disorder as a function of doping: (a) total energetic disorder; (b) additional disorder due to doping; (c) theoretical doping-induced disorder, that would exist if intrinsic and extrinsic disorders were not correlated, as a function of the dopant molar ratio (MR).

References

- [1] A. Miller, E. Abrahams, *Phys. Rev.* **1960**, *120*, 745.
- [2] R. A. Marcus, *J. Chem. Phys.* **1956**, *24*, 966.
- [3] A. Fediai, F. Symalla, P. Friederich, W. Wenzel, *Nat. Commun.* **2019**, *10*, 1.